Multimedia Tools and Applications (2019) 78:23003–23027
https://doi.org/10.1007/s11042-019-7515-6

Image segmentation using multilevel thresholding based on modified bird mating optimization

Maliheh Ahmadi[1] · Kamran Kazemi[1] · Ardalan Aarabi[2,3] · Taher Niknam[1] · Mohammad Sadegh Helfroush[1]

Received: 12 July 2018 / Revised: 24 January 2019 / Accepted: 18 March 2019 /
Published online: 27 April 2019

Abstract
Multilevel thresholding using Otsu or Kapur methods is widely used in the context of image segmentation. These methods select optimal thresholds in gray level images by maximizing between-class variance or entropy criterion. These methods become time consuming and less efficient with increasing number of thresholds. To increase the efficiency of the image segmentation using multilevel thresholding based on Kapur and Otsu methods, we developed a hybrid optimization algorithm named BMO-DE based on bird mating optimization (BMO) and differential evolutionary (DE) algorithms. The efficiency of the proposed method was evaluated on eight standard benchmark images. The proposed method achieved better segmentation results in term of solution quality and stability in comparison with other well-known techniques including bacterial foraging (BF), modified bacterial foraging (MBF), particle swarm optimization (PSO), genetic algorithm (GA) and hybrid algorithm named PSO-DE.

Keywords Image segmentation · Multilevel thresholding · Bird mating optimization · Differential evolutionary

1 Introduction

Image segmentation is the process of partitioning an image into a number of homogenous regions, each containing pixels with similar attributes like intensity or texture. It is considered as an important pre-processing step in applications such as object detection and tracking, and medical image analysis [8, 12, 22, 29, 31, 37, 39, 40, 46, 48]. One of the widely used methods

✉ Kamran Kazemi
kazemi@sutech.ac.ir

[1] Department of Electrical and Electronics Engineering, Shiraz University of Technology, Shiraz, Iran

[2] Laboratory of Functional Neuroscience and Pathologies (LFNP, EA4559), University Research Center (CURS), CHU AMIENS - SITE SUD, Avenue Laënnec, 80420 Salouël, France

[3] Faculty of Medicine, University of Picardie Jules Verne, 80036 Amiens, France

for image segmentation is thresholding. It can be classified into bi-level and multilevel thresholding depending on the number of regions. In bi-level thresholding, the image pixels are classified into two regions, with gray levels greater or less than a certain threshold. In multilevel thresholding, an input image is segmented into several distinct regions with multiple thresholds [3, 7, 17, 22]. As an efficient tool, histogram thresholding can be used for image segmentation. However, finding the exact location of valleys in a multimodal histogram is not trivial.

The optimal thresholds in bi-level or multilevel thresholding can be determined using parametric or non-parametric approaches [14]. In the parametric approach, a probability density function is assigned to each class (region) with the distribution parameters computed by using the least-squares methods. In the non-parametric approaches, the thresholding method searches for optimal thresholds in the histogram by optimizing an objective function based on some criteria such as between-class variance (Otsu' [28]) or entropy [19]. However, all of these methods are computationally complex and less efficient due to the exhaustive search especially when the number of thresholds increases.

Recently, evolutionary algorithms inspired by biological evolution have been combined with multilevel thresholding algorithms such as Genetic Algorithm (GA) [11], Particle swarm optimization (PSO) [9, 13, 18, 26, 33, 44] bacterial foraging algorithm (BFO) [36, 37], differential evaluation (DE) [34, 43], artificial bee colony (ABC) [2, 16], cuckoo search (CS) [1, 32], watershed algorithm [47], fuzzy logic [24], hybrid method [30], honey bee mating optimization (HBMO) [15], wind driven optimization (WDO) [5], self-adaptive parameter optimization [23], grey wolf optimizer (GWO) [20], Whale Optimization Algorithm (WOA) and Moth-Flame Optimization (MFO) [10] for optimal multilevel thresholding. The multilevel thresholding using evolutionary algorithms have been applied in various applications including brain tissue segmentation from magnetic resonance images [21, 25, 38, 41] and satellite hyper-spectral image segmentation [6, 35]. Among all the multilevel thresholding algorithms, GA, PSO and BFO have shown good segmentation results with significant reduced computational cost for multilevel thresholding using Otsu criterion or Kapur's entropy.

Although the evolutionary algorithms provide promising results for finding optimal thresholds in comparison with the parametric approaches, most of them exhibits slow convergence and may get trapped in local minima highly affecting their quality of segmentation [20]. The hybridization of the evolutionary methods is a practical solution to overcome this limitation by improving their efficiency in terms of convergence speed and solution quality.

Recently, Askarzadeh [4] proposed the bird mating optimization (BMO) algorithm, a population based method based on bird mating phenomenon, in which each bird attempts to breed a quality brood as much as possible. BMO employs distinct patterns to move through the search space without being trapped in local extrema. Thus, it can explore the search space and generate new solutions while maintaining the population diversity. Although BMO presents promising results in solving optimization problems, it is still inefficient in terms of convergence speed and quality of solution [49]. In order to improve the quality of the BMO solution, we introduce a hybrid algorithm (called BMO-DE) based on BMO and the differential evolutionary (DE) algorithm. DE is an easy-to-use general search algorithm with a simple structure holding acceptable convergence properties; however it may get trapped in local minima. The proposed hybrid algorithm BMO-DE was used to efficiently solve the multilevel thresholding problem for image segmentation by using the objective functions of Kapur's and Otsu's methods.

The paper is organized as follows: Section 2 presents the Kapur's and Otsu's methods for multilevel thresholding. Section 3 gives an overview of the BMO, DE and proposed hybrid BMO-DE algorithms. The application of the proposed BMO-DE algorithm for multilevel thresholding is presented in Section 4. Finally, performance evaluation and conclusion are given in sections 5 and 6, respectively.

2 Optimal thresholding methods

Suppose a given image has N pixels and L gray levels over [0, L-1]. The probability of gray level i is given as follows:

$$P_i = \frac{f_i}{N}, \quad N = \sum_{i=0}^{L-1} f_i, \quad i = 0, 1, ..., L-1 \tag{1}$$

Where f_i is the number of pixels with gray level i. In optimal thresholding methods optimal thresholds are found such that the segmented classes satisfy desired properties. We used the entropy criterion (Kapur's) and between-class variance (Otsu's) method to perform image segmentation via multilevel thresholding.

2.1 Entropy criterion method

The Kapur's method for image thresholding maximizes the posterior entropy by measuring the homogeneity of image regions [19, 45]. According to this criterion, the objective function based on bi-level thresholding is described as follows:

$$fit(x) = H_1 + H_2 \tag{2}$$

where

$$\begin{aligned} H_1 &= -\sum_{i=0}^{x-1} \frac{P_i}{w_1} \ln \frac{P_i}{w_1}, \quad w_1 = \sum_{i=0}^{x-1} P_i \\ H_2 &= -\sum_{i=x}^{L-1} \frac{P_i}{w_2} \ln \frac{P_i}{w_2}, \quad w_2 = \sum_{i=x}^{L-1} P_i \end{aligned} \tag{3}$$

Gray level that maximizes eq. 2 is considered as the optimal threshold x.

The Kapur's method can be extended to multilevel thresholding to find c thresholds $X = [x_1, x_2, ..., x_c]$ by maximizing the following objective function:

$$fit(X) = H_1 + H_2 + ... + H_c \tag{4}$$

where

$$\begin{aligned} H_1 &= -\sum_{i=0}^{x_1-1} \frac{P_i}{w_1} \ln \frac{P_i}{w_1}, \; w_1 = \sum_{i=0}^{x_1-1} P_i \\ H_2 &= -\sum_{i=x_1}^{x_2-1} \frac{P_i}{w_2} \ln \frac{P_i}{w_2}, \; w_2 = \sum_{i=x_1}^{x_2-1} P_i \\ &\vdots \\ H_c &= -\sum_{i=x_c}^{L-1} \frac{P_i}{w_c} \ln \frac{P_i}{w_c}, \; w_c = \sum_{i=x_c}^{L-1} P_i \end{aligned} \tag{5}$$

where H_1, H_2, ..., $H_c$are the Kapur's entropies and w_1, w_2, ..., $w_c$are the probabilities of the segmented classes.

2.2 Between-class variance method

Otus's method selects the optimal threshold at level$x$, which maximizes the between-class variance. According to this threshold, the input image is divided into two classes: C_1 and C_2; where class C_1includes gray levels from 0 to $x-1$ and class C_2 consists of gray levels from x to $L-1$. The cumulative probabilities w_1 and w_2, and the mean gray levels μ_1 and μ_2 for classes C_1 and $C_2$are defined as follows:

$$w_1 = \sum_{i=0}^{x-1} P_i, \quad \mu_1 = \sum_{i=0}^{x-1} i \times \frac{P_i}{w_1} \tag{6}$$

$$w_2 = \sum_{i=x}^{L-1} P_i, \quad \mu_2 = \sum_{i=x}^{L-1} i \times \frac{P_i}{w_2} \tag{7}$$

The optimum threshold is selected in a way that maximizes the objective function:

$$fit(x) = \sigma_1 + \sigma_2 \tag{8}$$

where

$$\sigma_1 = w_1(\mu_1 - \mu_{Total})^2, \quad \sigma_2 = w_2(\mu_2 - \mu_{Total})^2 \tag{9}$$

and μ_{Total} is the mean intensity of the whole image defined as follows:

$$\mu_{Total} = w_1\mu_1 + w_2\mu_2 \tag{10}$$

This process can be extended to multilevel thresholding:

$$fit(X) = \sigma_1 + \sigma_2 + ... + \sigma_c \tag{11}$$

where

$$\begin{aligned} \sigma_1 &= w_1(\mu_1 - \mu_{Total})^2, \\ \sigma_2 &= w_2(\mu_2 - \mu_{Total})^2, \\ &\vdots \\ \sigma_c &= w_c(\mu_c - \mu_{Total})^2 \end{aligned} \tag{12}$$

and c thresholds are defined as $X = [x_1, x_2, ..., x_c]$.

3 Proposed BMO-DE method

3.1 Bird mating optimization (BMO)

BMO is a meta-heuristic optimization algorithm based on mating behavior of birds. In this algorithm the population is called society and each member of the society is named bird, which

represents a feasible solution. The society has two parts consisting of males and females. The birds in the society are responsible to breed a quality brood as much as possible. The female birds are classified into parthenogenetics and polyandrous. The males are divided into three groups namely monogamous, polygynous and promiscuous. According to the mating pattern of the birds, BMO possesses five updating patterns, each of them has different updating phase and produces a solution as described below [4].

Monogamy is a mating system that a male bird mates with one female. Each monogamous bird selects an interesting female by evaluating the quality of the female birds in a probabilistic approach and mates with her. The chance of each female depends on promising gens of that female. In this system the new offspring brood is generated as follows:

$$\begin{aligned}
&\overrightarrow{X}_b = \overrightarrow{X} + W \times \overrightarrow{r} \times \left(\overrightarrow{X}^l - \overrightarrow{X}\right)\\
&for\ m = 1\ to\ c\\
&if\ r_1 > mcf\\
&\quad X_b(m) = lb(m) - r_2 \times (lb(m) - ub(m))\\
&else\\
&\quad X_b(m) = X(m);\\
&\ end\ if\\
&end\ for
\end{aligned} \tag{13}$$

The first part of Eq. 13 shows that by combining the monogamous bird $\overrightarrow{X}$ with the interesting female $\overrightarrow{X}^l$, the new brood $\overrightarrow{X}_b$ inherits the good genes from his parents. In this equation, W is a time-varying weight showing the role of the interesting female on each of the offspring broods. $\overrightarrow{r}$ denotes a c dimensional vector, in which each element has a uniform distribution between 0 and 1, and c is the dimension of the problem. The second part of the Eq. 13 defines the mutation operation in one of the brood's genes with the probability of $1 - mcf$, where lb and ub are lower and upper bounds of the dimension of the problem and r_n is a random variable between 0 and 1.

Polygyny indicates a mating system that polygynous bird mates with several female birds to have better genes for the brood. The new offspring brood is calculated as below:

$$\begin{aligned}
&\overrightarrow{X}_b = \overrightarrow{X} + W \times \sum_{k=1}^{nl} \overrightarrow{r}_k \times \left(\overrightarrow{X}_k^l - \overrightarrow{X}\right)\\
&for\ m = 1\ to\ c\\
&\ if\ r_1 > mcf\\
&\quad X_b(m) = lb(m) - r_2 \times (lb(m) - ub(m))\\
&\ else\\
&\quad X_b(m) = X(m);\\
&\ end\ if\\
&end\ for
\end{aligned} \tag{14}$$

where n_l is the number of interesting female birds.

Promiscuity is a mating system in which two birds have unstable relationships. This mating presents a chaotic sequence. In this system a male bird mates with one female according to Eq. 13.

Parthenogenesis is another mating system that each female can raise brood without the help of males. By making a small change in genes of each female the offspring brood is generated as follows:

$$\begin{aligned} &for\ m = 1\ to\ c \\ &\ if\ r_1 > mcfp \\ &\ \ X_b(m) = X(m) + mu \times (r_2 - r_3) \times X(m); \\ &else \\ &\ \ X_b(m) = X(m); \\ &\ end\ if \\ &end\ for \end{aligned} \tag{15}$$

where *mcfp* and *mu* are the mutation control factor and the step size, respectively.

Polyandry implies a mating system that a female bird mates with several males. The polyandrous bird choices monogamous males probabilistically. The brood is generated using Eq. 14.

3.2 Differential evolution (DE)

The differential evolution (DE) algorithm is an evolutionary optimization technique introduced by Storn and Price in 1995 [42]. DE with good global search ability uses crossover and mutation operators like GA but with different mechanism. In c dimensional search spaces, each individual in the DE population is produced by $X_j = (x_{j,\,1},\ \ldots, x_{j,\,c})$ from the feasible solution space. At each generation, mutant vectors (X_{mut}, X_{mut1}, X_{mut2} *and* X_{mut3}) are generated for each individual according to the following three strategies:

$$\begin{aligned} X_{mut} &= X_{p0} + F_1 \times \left(X_{p1} - X_{p2}\right) \\ X_{mut\,1} &= X_{p0} + F_1 \times \left(X_{p1} - X_{p2}\right) + F_2 \times \left(X_{best} - X_{worst}\right) \\ X_{mut2} &= F_3 \times \left(X_{best} - X_{worst}\right) + X_{p3} \\ X_{mut3} &= X_{p0} + F_1 \times \left(X_{p4} - X_{p3}\right) \end{aligned} \tag{16}$$

where $p0, p1, p2, p3$ and $p4$ are the different random integer numbers from $[1, N_{pop}]$ and N_{pop} is the size of the population. In order to adjust the difference vectors F_1, F_2 and F_3 are chosen as scaling factors selected randomly by using normal distribution.

After applying mutation, trial vectors X_{new}, X_{new1}, X_{new2} *and* X_{new3} named crossover vectors are produced by crossover operation based on $X_j$and X_{mut}, X_{mut1}, X_{mut2}, *and* X_{mut3} vectors as:

$$\begin{aligned} x_{new,m} &= \begin{cases} x_{mut1,m} & if\ rand < CR\ or\ m = z \\ x_{j,m} & otherwise \end{cases} \\ x_{new1,m} &= \begin{cases} x_{mut3,m} & if\ rand < CR1\ or\ m = z \\ x_{j,m} & otherwise \end{cases} \\ x_{new2,m} &= \begin{cases} x_{mut,m} & if\ rand < CR2\ or\ m = z \\ x_{mut2,m} & otherwise \end{cases} \\ x_{new3,m} &= \begin{cases} x_{mut,m} & if\ rand < CR3\ or\ m = z \\ x_{mut1,m} & otherwise \end{cases} \\ m &= 1 \ldots c \end{aligned} \tag{17}$$

where $x_{j,\,m}$ and $x_{new,\,m}$, $x_{new1,\,m}$, $x_{new2,\,m}$, $x_{new3,\,m}$ are the m^{th} dimensional components of the vectors X_j and x_{new}, x_{new1}, x_{new2}, x_{new3}, respectively. CR, $CR1$, $CR2$ *and* $CR3$ are the crossover constants, which are usually set to fixed values within (0,1); z is an integer number that is

randomly chosen from the index set $\{1, 2, ..., c\}$, which makes sure crossover vectors get at least one parameter from mutant vectors.

3.3 Hybrid BMO-DE algorithm

The proposed hybrid evolutionary algorithm (called BMO-DE) was developed by integrating DE into BMO for updating population (society). We used DE to improve the solution quality of the BMO algorithm. The proposed hybrid algorithm was implemented as follows:

Step 1: Initialization: an initial society S is randomly generated as $S = [X_1, X_2, ..., X_{N_{pop}}]$ where $X_j = [x_1, ...x_c]$ represents the j^{th} bird in the society.
Step 2: Fitness function: in this step, a constrained optimization problem with regard to predefined variables should be solved:

$$Fit(X) = fit(X) - k_1\left(\sum_{a=1}^{N_{eq}} (h_a(X))^2\right) - k_2\left(\sum_{b=1}^{Nueq} (Max[0, -g_b(X)])^2\right) \quad (18)$$

where $fit(X)$ is the objective function; N_{eq} and N_{ueq} are the number of equality and inequality constraints of the problem, respectively; $h_a(X)$ *for* $a = 1, ..., N_{eq}$ and $g_b(X)$ *for* $b = 1, ..., N_{ueq}$ are constraints that should be fulfilled; and k_1 and k_2 are the penalty coefficients that are set in order to meet the constraints. If there are no constraints in the problem, the penalty coefficients are set to zero and the value of the fitness function $Fit(X)$ and the objective function $fit(X)$ are equal.

Step 3: Ranking and classification: the birds in the society are ranked and classified into two groups (male and female) according to their fitness function. The females are equally divided into two groups as parthenogenetic and polyandrous birds. The males are categorized into three groups called monogamous, polygynous and promiscuous.
Step 4: Breeding: select the j^{th} bird and calculate a brood using its pattern.
Step 5: Replacement: replace the new brood with its own bird if it has a better quality.
Step 6: Hybrid BMO-DE: apply the DE to the j^{th} brood of the monogamous or polygynous birds. If the quality of the DE mutant vector is better than its own brood, the brood abandons the society and the DE vector is joined to the society as a new brood**.**
Step 7: repeat steps 4–6 until all birds are evaluated.
Step 8: if the termination criterion is satisfied, stop the search procedure. Otherwise, replace the initial population with the current population and go back to step 3.
Step 9: the bird with the best quality is selected from the society as the final solution.

The flowchart of the hybrid BMO-DE is illustrated in Fig. 1.

4 Image segmentation using the proposed BMO-DE

In the society of birds, they are responsible to breed a quality brood with superior genes. In the multilevel thresholding problem, the proposed BMO-DE algorithm is applied to imitate the behaviour of birds to breed broods (optimal threshold values) that optimize objective functions

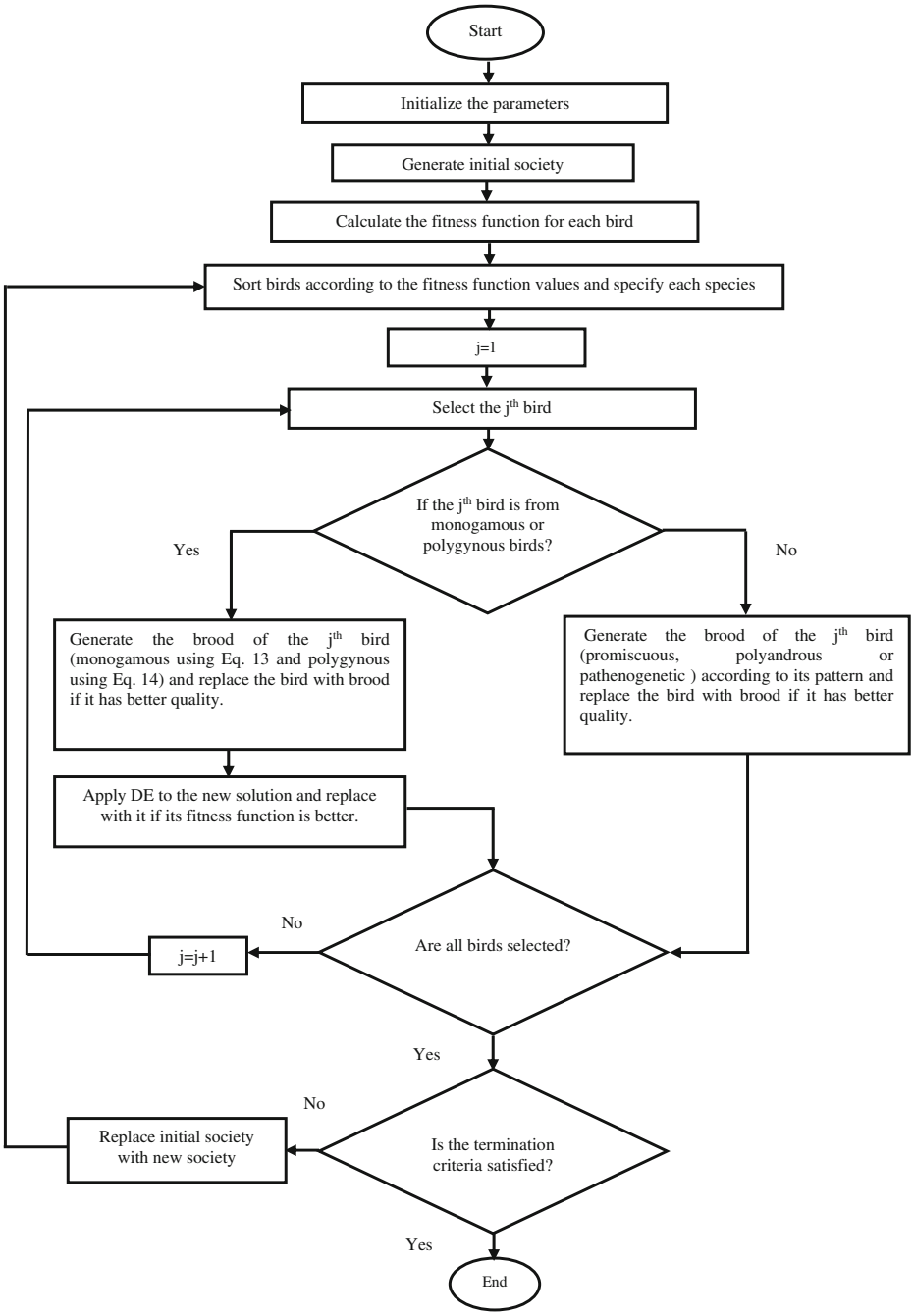

Fig. 1 The flowchart of the proposed hybrid BMO-DE algorithm

given by Eqs. 4 or 11. The image histogram is the input of this algorithm and the optimal bird $\overrightarrow{X}_b$, which represents the optimal threshold is the output.

Suppose that to find c thresholds for the segmentation problem, the search space is c-dimensional and the j^{th} bird can be represented by a c-dimensional vector$X_j = [x_{j,\ 1},\ x_{j,\ 2}, ..., x_{j,\ c}]$ of the possible real values corresponding to the thresholds. In the first stage of the proposed multilevel thresholding method, an initial society consisting of N_{pop} vectors $X_j = [x_{j,\ 1}, x_{j,\ 2}, ..., x_{j,\ c}]$, $j = 1,\ ...,\ N_{pop}$ is generated randomly as birds according to Eq. 19:

$$x_{j,k} = rand(.) \times \left(x_{\max,k} - x_{\min,k}\right) + x_{\min,k} \tag{19}$$

Where $x_{\min,\ k}$ and $x_{\max,\ k}$ are the minimum and maximum of the gray levels in the input image and the birds $X_j = [x_{j,\ 1}, x_{j,\ 2}, ..., x_{j,\ c}]$ (thresholds) are initialized within this range. Each bird with length c is a feasible solution of the thresholding problem. The fitness function is used to assess the quality of each bird X_j. Since there are no constraints in our problem, the objective function and fitness function in Eq. 18 are the same. Therefore, the fitness function is calculated based on Kapur's entropy (Eq. 4) or Otsu's criterion (Eq. 11) for each bird X_j in the society.

In the second stage, the birds of the society (thresholds) are sorted based on their quality (value of fitness function) and they are classified into males and females. The females are those birds that have promising genes (i.e. the most fitness function value) and they are equally divided into two groups: *i)* parthenogenetic group with better genes (better thresholds) and *ii)* polyandrous group. On the other hand, the males are categorized into three groups (step 3 in subsection 3.3). The better ones make the first group named monogamous and the birds in the second group are named polygynous. The birds in the third group, named promiscuous, have the worse quality (worse threshold) are excluded from the society and replaced with ones that are generated using a chaotic sequence. Each bird as an optimal threshold breeds a brood according to its pattern (Eqs. 13 to 15). The bird (threshold in the previous iteration) can be replaced with its own brood (threshold in the new iteration) if the quality of the brood is better, in other words, it has a fitness function value greater than that of its parent.

In the third stage, DE is applied to each brood of the monogamous or polygynous birds based on Eqs. 16 and 17. If the fitness function value of the DE mutant vector is better than that of its own brood, the brood is updated with the DE vector. The search procedure is repeated until the termination criterion is satisfied. The bird X_j with the best quality, a vector consisting of c thresholds, represents the final solution of the multilevel thresholding problem.

5 Performance evaluation

The performance of the proposed method and that of other well-known methods including PSO, GA, BF, MBF [37] and hybrid PSO-DE algorithm [27] was evaluated on standard test images: Lena, Peppers, Baboon, Hunter, Cameraman, Living room, Airplane and Butterfly. The original images and their corresponding histograms are shown in Fig. 2. The proposed BMO-DE based multilevel thresholding method was implemented in MATLAB using a Pentium(R) Dual core 2.30 GHz and 2 GB of memory. The mean and standard deviation of the objective function values as well as

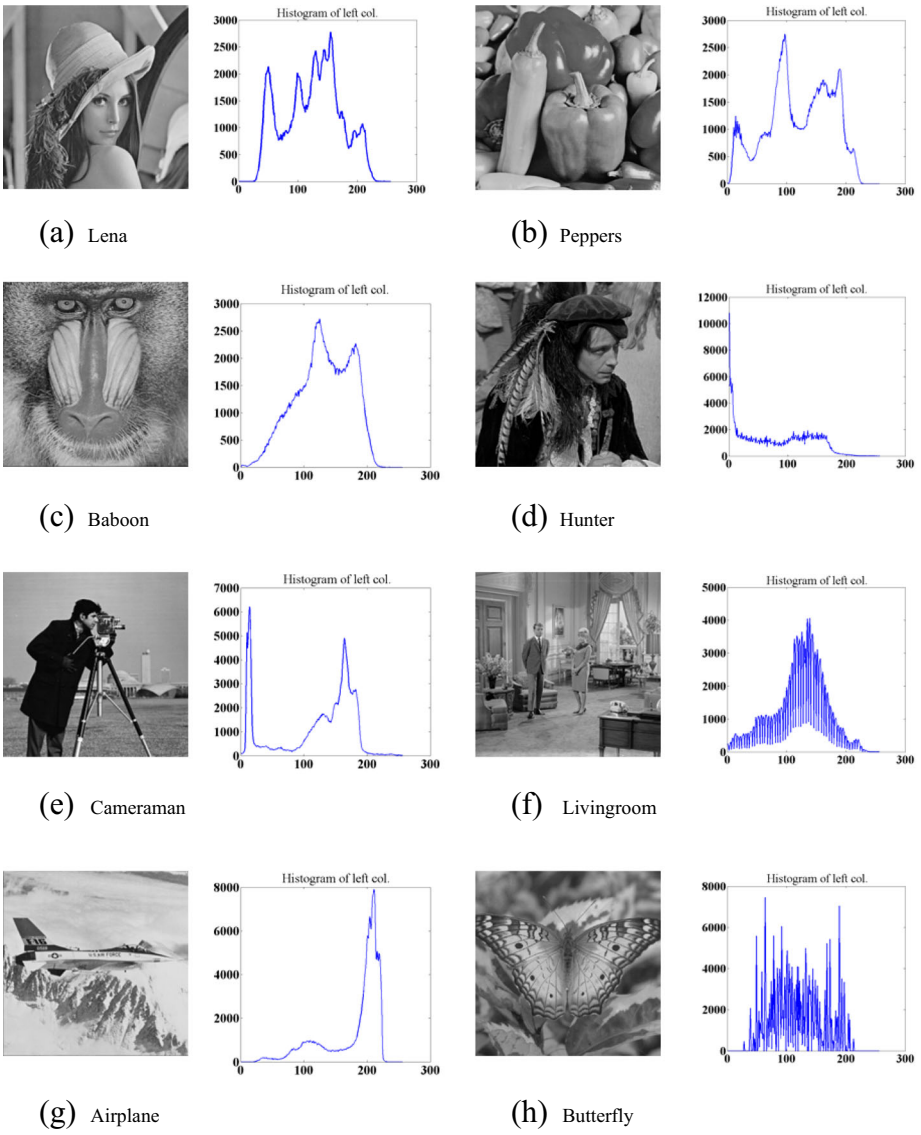

Fig. 2 Original gray level test images and the corresponding histograms that are used to perform experiments. The size of images are 512 × 512. (a) Lena, (b) Peppers, (c) Baboon, (d) Hunter, (e) Cameraman, (f) Living room, (g) Airplane and (h) Butterfly

the corresponding CPU time were reported within a range of thresholds for each multilevel thresholding method included in the study.

5.1 Segmentation result

Figures 3 and 4 show the segmentation results obtained by the proposed BMO-DE methods based on Kapur's entropy and Otsu criteria using three thresholds, respectively. As shown, the segmentation accuracy was improved significantly with increasing the number of thresholds.

5.2 Solution quality

Tables 1 and 2 show the mean (± std) objective values obtained using both Otsu's and Kapur's objective functions for BMO-DE, PSO-DE, GA, PSO, BF and MBF. The corresponding threshold values are shown in Tables 3 and 4. In order to evaluate the stability of the

Fig. 3 Segmentation of test images using the proposed BMO-DE-Kapur multilevel thresholding method. The first, second and third columns represent the segmented image into four (c = 3), five (c = 4) and six (c = 5) regions, respectively. From top to bottom: Lena, Peppers, Baboon, Hunter, Cameraman, Living room, Airplane and Butterfly

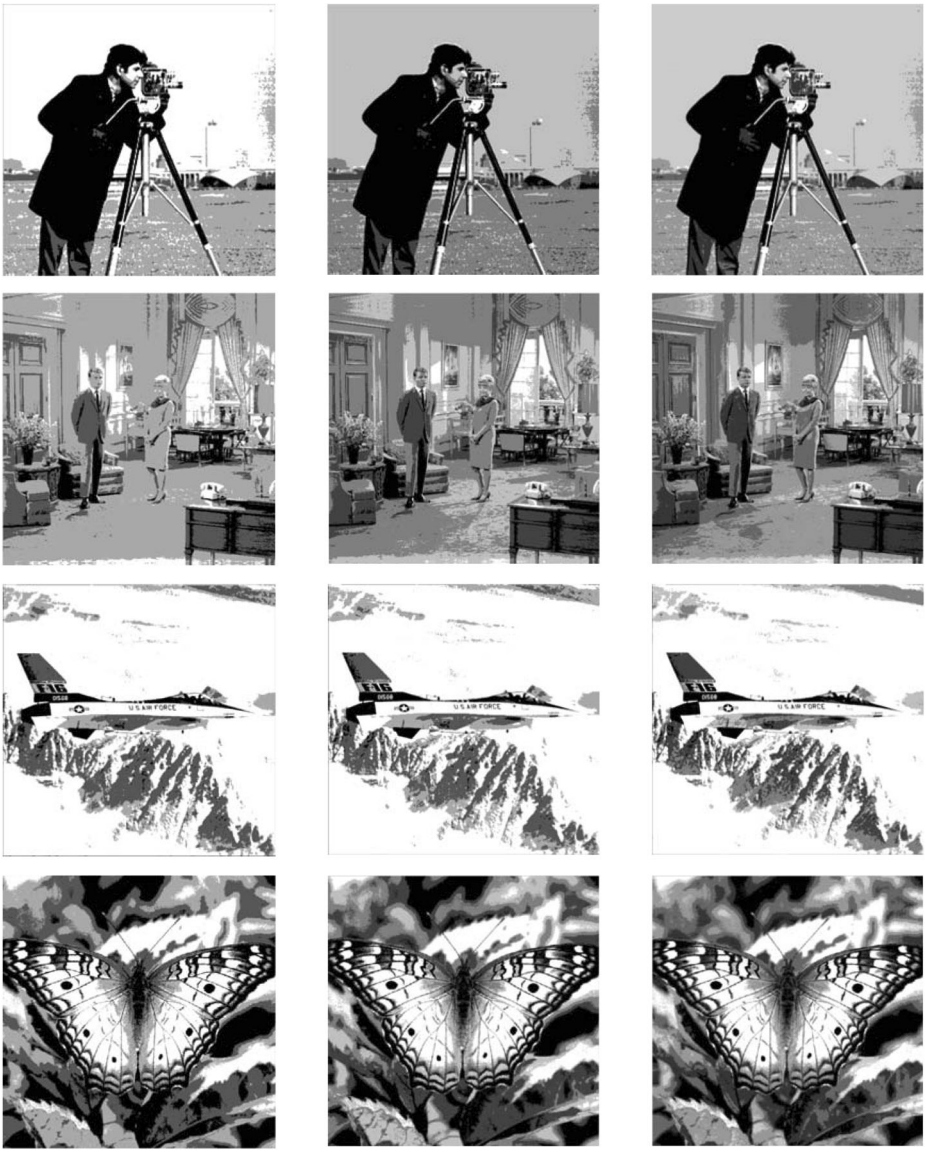

(continued)

evolutionary methods for multilevel thresholding we computed the standard deviation (std) of their objective function values over K runs as follows [37]:

$$std = \sqrt{\sum_{a=1}^{K} \frac{(\delta_a - \mu)}{K}} \tag{20}$$

where K is number of runs for each algorithm, $\delta_a$is the best objective value obtained by the a^{th} run of the algorithm, and μ is the mean value of δ. A lower standard deviation indicates higher

stability for the algorithm. We evaluated the stability of the evolutionary algorithms over 50 runs ($K = 50$). As shown in Tables 1 and 2, the proposed method exhibited higher stability in comparison with other methods using both Otsu's and Kapur's objective functions. We also performed a

Fig. 4 Segmentation of test images using the proposed BMO-DE-Otsu multilevel thresholding method. The first, second and third columns represent the segmented image into four (c = 3), five (c = 4) and six (c = 5) regions, respectively. From top to bottom: Lena, Peppers, Baboon, Hunter, Cameraman, Living room, Airplane and Butterfly

(continued)

statistical analysis using t-test at a significance level of 0.05 to assess the significant differences between the objective values of the proposed algorithm and those of PSO-DE, MBF, BF, PSO and GA over the runs. The statistical differences ($P < 0.05$) between our algorithm and each of the other approaches are shown by asterisks in Tables 1 and 2. Moreover, in most cases our method yielded higher values using both Otsu's and Kapur's objective functions. The Kapur based PSO-DE algorithm, however, showed a comparable accuracy to that of our method.

Table 1 The mean and std. of objective function values for different threshold levels (c = 2,3,4,5) obtained by Kapur based BMO-DE, PSO-DE, MBF, BF, PSO and GA algorithms. The asterisks show statistical differences between our algorithm and each of the other approaches using t-test at a significance level of 0.05

Test images	c	BMO-DE	PSO-DE	MBF	BF	PSO	GA
Lena	2	12.3464 ± 3.59E-15	12.3301 ± 0.0113	12.347 ± 1.24E–04	12.3470 ± 2.99E–04	12.3459 ± 0.0033	12.3344 ± 0.0049
	3	15.5244 ± 5.38E-15	15.4246 ± 0.0741*	15.2784 ± 0.0041*	15.2206 ± 0.0061*	15.1336 ± 0.0390*	14.9956 ± 0.1100*
	4	18.4964 ± 9.17E-06	18.438 ± 0.0553	17.9598 ± 0.0069*	17.9333 ± 0.0081*	17.8388 ± 0.0081*	17.0892 ± 0.2594*
	5	21.1827 ± 0.0068	21.1446 ± 0.0390	20.6106 ± 0.0319*	20.6099 ± 0.0502*	20.4427 ± 0.2181*	19.5492 ± 0.3043*
Peppers	2	12.6346 ± 0	12.6283 ± 0.0051	12.5198 ± 2.2E–04*	12.5191 ± 4.08E–04*	12.5168 ± 0.0012*	12.5133 ± 0.0031*
	3	15.6887 ± 8.97E-15	15.6861 ± 0.0022	15.4866 ± 0.0236*	15.3998 ± 0.0324*	15.0939 ± 0.0764*	14.7122 ± 0.1750*
	4	18.5369 ± 0.0060	18.5247 ± 0.0144	18.2774 ± 0.0020*	18.2697 ± 0.0465*	18.0974 ± 0.1080*	17.6959 ± 0.2707*
	5	21.2687 ± 0.0154	21.2784 ± 0.0015	21.0468 ± 0.0090	20.9999 ± 0.0181*	20.7338 ± 0.1758*	20.0691 ± 0.3048*
Baboon	2	12.2395 ± 0	12.2339 ± 0.0037	12.2168 ± 1.01E–04*	12.2164 ± 8.88E–04*	12.2134 ± 0.0077*	12.1847 ± 0.0567
	3	15.3135 ± 0.0001	15.3090 ± 0.0025	15.2643 ± 0.0155*	15.2114 ± 0.0287*	15.0088 ± 0.0816*	14.7457 ± 0.1580*
	4	18.1752 ± 0.0017	18.1741 ± 0.0012	18.0278 ± 0.0186*	17.9992 ± 0.0336*	17.5743 ± 0.0853*	16.9356 ± 0.1765*
	5	20.8364 ± 0.0118	20.8450 ± 0.0016	20.7881 ± 0.0172	20.7200 ± 0.1065*	20.2245 ± 0.1899*	19.6622 ± 0.2775*
Hunter	2	12.3762 ± 0	12.3485 ± 0.0166	12.3774 ± 0.0010	12.3733 ± 0.0033	12.3708 ± 0.0068	12.3496 ± 0.0148
	3	15.6124 ± 6.69E-05	15.6075 ± 0.0040	15.5880 ± 0.111	15.5533 ± 0.1155	15.1286 ± 0.0936*	14.8381 ± 0.1741*
	4	18.5246 ± 0.0023	18.5232 ± 0.0019	18.3932 ± 0.0032*	18.3819 ± 0.0055*	18.0401 ± 0.1560*	17.3189 ± 0.2192*
	5	21.2112 ± 0.0216	21.2229 ± 0.0088	21.2629 ± 0.0018	21.2565 ± 0.0029*	20.5339 ± 0.2720*	19.5635 ± 0.3466*
Cameraman	2	12.2717 ± 1.79E-15	12.2426 ± 0.0264	12.2794 ± 0.0015	12.2646 ± 0.0041	12.2595 ± 0.1001	11.9414 ± 0.1270*
	3	15.3795 ± 1.61E-14	15.3629 ± 0.0213	15.2705 ± 0.0040*	15.2507 ± 0.0075*	15.2110 ± 0.1107*	14.8278 ± 0.2136*
	4	18.5403 ± 0.0045	18.5401 ± 0.0007	18.4321 ± 0.0063*	18.4066 ± 0.0081*	18.0009 ± 0.2005*	17.1665 ± 0.2857*
	5	21.2956 ± 0.0191	21.3034 ± 0.0064	21.2259 ± 0.0044*	21.2111 ± 0.0741	20.9631 ± 0.2734*	19.7950 ± 0.3528*
Livingroom	2	12.4056 ± 9.13E-05	12.3939 ± 0.0077	12.406 ± 8.3E–05	12.4057 ± 0.0018	12.4000 ± 0.0022	12.3923 ± 0.0039
	3	15.5523 ± 1.08E-14	15.5361 ± 0.0073	15.4374 ± 0.0063*	15.4077 ± 0.0089*	15.2123 ± 0.0718*	14.9700 ± 0.1364*
	4	18.4654 ± 0.0062	18.4604 ± 0.0039	18.3970 ± 0.0091*	18.3194 ± 0.0871*	18.1410 ± 0.2286*	17.2063 ± 0.3220*
	5	21.1220 ± 0.0209	21.1327 ± 0.0038	21.1275 ± 0.0210	21.1198 ± 0.0820	20.6752 ± 0.2619*	19.8410 ± 0.3805*
Airplane	2	12.1761 ± 7.18E-15	12.1665 ± 0.0062	12.1761 ± 5.8E–05	12.1759 ± 0.0076	12.1503 ± 0.0106	12.1153 ± 0.0305*
	3	15.4333 ± 1.97E-14	15.4300 ± 0.003	15.3736 ± 0.0033*	15.3605 ± 0.0062*	15.2925 ± 0.1248*	14.8059 ± 0.1958*
	4	18.4290 ± 1.07E-05	18.2753 ± 0.0731*	18.1876 ± 0.0042*	18.1777 ± 0.0484*	18.0300 ± 0.1424*	17.8923 ± 0.3011*
	5	21.1979 ± 0.0045	21.1595 ± 0.0540	20.7695 ± 0.0054*	20.7515 ± 0.0188*	20.3964 ± 0.2760*	19.4465 ± 0.3369*
Butterfly	2	11.0843 ± 1.08E-14	10.7946 ± 0.2599*	10.4761 ± 1.89E–04*	10.4749 ± 0.0014*	10.4743 ± 0.0025*	10.4707 ± 0.0872*
	3	13.7719 ± 3.59E-15	13.6848 ± 0.0745*	12.7622 ± 0.0015*	12.7546 ± 0.0118*	12.3130 ± 0.1880*	11.6280 ± 0.2021*
	4	16.1089 ± 9.37E-05	16.0309 ± 0.0698	14.9118 ± 0.0099*	14.8777 ± 0.0166*	14.2317 ± 0.2473*	13.3144 ± 0.2596*
	5	18.2127 ± 0.0065	18.1962 ± 0.0147	16.8376 ± 0.0300*	16.8282 ± 0.0887*	16.3374 ± 0.2821*	15.7566 ± 0.3977*

Table 2 The mean and std. of objective function values at 50 runs for different threshold levels (c = 2,3,4,5) obtained by Otsu based BMO-DE, PSO-DE, MBF, BF, PSO and GA algorithms. The asterisks show statistical differences between our algorithm and each of the other approaches using t-test at a significance level of 0.05

Test images	c	BMO-DE	PSO-DE	MBF	BF	PSO	GA
Lena	2	1961.7603 ± 4.59E-13	1958.253 ± 2.7694*	1961.5822 ± 0.0064*	1961.5556 ± 0.0390*	1961.4149 ± 0.1423*	1960.9603 ± 0.2077*
	3	2128.2839 ± 2.76E-12	2127.241 ± 0.8147*	2128.2683 ± 0.0473	2128.0706 ± 0.0750*	2127.7771 ± 0.4155*	2126.4107 ± 0.5555*
	4	2191.7753 ± 0.1183	2191.342 ± 0.3879*	2191.6014 ± 0.4283	2189.0267 ± 0.7305*	2180.6868 ± 2.3601*	2173.7148 ± 3.0640*
	5	2217.0033 ± 0.5429	2216.886 ± 0.4055	2217.5366 ± 0.6492*	2215.6092 ± 2.7184*	2212.5555 ± 4.5341*	2196.2745 ± 5.7362*
Peppers	2	2532.3214 ± 9.19E-13	2529.006 ± 2.4189*	2475.7445 ± 0.0091*	2474.8090 ± 0.0111*	2469.5788 ± 0.0956*	2457.1517 ± 0.1455*
	3	2703.5715 ± 2.30E-12	2702.822 ± 0.5650*	2628.5874 ± 0.0175*	2625.3627 ± 0.0605*	2623.2739 ± 0.1629*	2614.0841 ± 0.2891*
	4	2766.2789 ± 0.3069	2765.568 ± 0.7635*	2698.8647 ± 0.2010*	2697.7838 ± 0.2468*	2695.8867 ± 2.1102*	2682.8391 ± 3.9721*
	5	2810.1130 ± 0.9029	2810.44 ± 0.2481	2737.5838 ± 0.2538*	2735.6447 ± 0.2711*	2733.5097 ± 3.2057*	2725.875 ± 4.9999*
Baboon	2	1561.7948 ± 1.61E-12	1557.098 ± 3.7768	1548.1408 ± 0.0368*	1548.0125 ± 0.0470*	1547.9977 ± 0.1040*	1547.6588 ± 0.2224*
	3	1653.4151 ± 0.0021	1652.616 ± 0.5072	1638.3205 ± 0.2438*	1637.0079 ± 0.3293*	1635.3623 ± 0.5720*	1633.5220 ± 1.5317*
	4	1707.3252 ± 0.1776	1707.144 ± 0.2103	1691.9499 ± 0.3469*	1690.722 ± 1.0655*	1684.3363 ± 2.1501*	1677.7052 ± 3.0653*
	5	1733.1664 ± 0.5505	1733.363 ± 0.1849	1717.8910 ± 0.4853*	1716.7283 ± 1.6105*	1712.9582 ± 3.4447*	1699.3909 ± 4.6721*
Hunter	2	3064.1360 ± 0.0000	3059.192 ± 4.8059*	3064.2112 ± 0.0215	3064.1188 ± 0.0266	3064.0688 ± 0.2282	3064.0156 ± 0.3283
	3	3213.3632 ± 9.19E-13	3211.587 ± 1.5365*	3213.7300 ± 0.0815	3213.4460 ± 0.3257	3212.0585 ± 0.8203*	3211.7947 ± 1.8080*
	4	3269.3486 ± 0.1561	3268.885 ± 0.3772	3269.5160 ± 0.7356	3266.3504 ± 2.2894*	3257.1767 ± 2.9836*	3231.1313 ± 6.3644*
	5	3307.2165 ± 0.8406	3306.917 ± 0.7342*	3296.3196 ± 1.3232*	3291.1339 ± 3.6102*	3276.3173 ± 7.3030*	3244.7387 ± 11.1247*
Cameraman	2	3608.4668 ± 3.67E-12	3599.459 ± 7.7635*	3609.5601 ± 0.0186	3609.4995 ± 0.0363*	3609.3703 ± 0.0908	3609.0761 ± 0.3812
	3	3682.1970 ± 0.0041	3681.156 ± 0.5544*	3683.3513 ± 0.2329	3682.5693 ± 1.4250	3677.1783 ± 6.3502*	3643.2153 ± 9.4711*
	4	3737.8699 ± 0.1985	3737.168 ± 0.5902	3739.2670 ± 0.5446	3737.1201 ± 1.5756*	3722.6447 ± 2.4498*	3710.7311 ± 4.5059*
	5	3768.0288 ± 0.6797	3768.357 ± 0.2382	3770.0122 ± 0.7447	3769.2239 ± 2.1916	3764.9571 ± 8.9650*	3755.5529 ± 11.0079*
Livingroom	2	1627.8690 ± 1.15E-12	1622.331 ± 4.5731*	1627.9092 ± 0.0180	1627.824 ± 0.0750	1627.7966 ± 0.2637	1627.0537 ± 0.5425*
	3	1760.0541 ± 6.89E-13	1758.495 ± 1.1585*	1760.103 ± 0.0716	1759.8457 ± 0.3475*	1757.4664 ± 1.0446*	1748.6885 ± 2.4428*
	4	1828.7235 ± 0.2011	1827.951 ± 0.5878*	1828.8644 ± 0.5010	1826.6284 ± 0.9089*	1822.1136 ± 2.0787*	1816.0692 ± 3.0313*
	5	1871.2333 ± 0.7327	1871.322 ± 0.4057*	1871.9906 ± 0.7778	1869.9966 ± 1.0430*	1865.4766 ± 2.2655*	1858.0959 ± 4.3189*
Airplane	2	1837.7974 ± 1.15E-12	1836.199 ± 1.4990*	1837.7974 ± 0.4320	1837.7517 ± 0.8861	1837.7222 ± 1.1731	1837.7144 ± 2.7001
	3	1911.7236 ± 2.07E-12	1911.087 ± 0.4511*	1911.7236 ± 0.5587	1910.7434 ± 1.6725*	1905.7664 ± 2.5107*	1844.5642 ± 5.0948*
	4	1954.9821 ± 0.129723	1954.68 ± 0.2726*	1955.0488 ± 0.8800	1954.248 ± 1.9995*	1953.8872 ± 3.4728*	1950.5919 ± 7.0157*
	5	1979.2602 ± 0.690713	1979.618 ± 0.2202	1979.9597 ± 1.3651	1978.4335 ± 2.0057*	1977.9742 ± 4.7571*	1973.0894 ± 8.6500*
Butterfly	2	1553.0734 ± 1.38E-12	1551.566 ± 1.8276*	1553.6825 ± 0.5099	1553.0734 ± 0.7817	1553.0687 ± 1.6744	1552.4129 ± 2.3493*
	3	1669.2783 ± 1.15E-12	1668.366 ± 0.8803*	1668.9174 ± 0.6469*	1667.2801 ± 1.2321*	1665.7589 ± 2.2356*	1662.6963 ± 3.4016*
	4	1711.2067 ± 0.0386	1710.724 ± 0.5133	1711.2193 ± 1.2898	1707.0994 ± 2.2632*	1702.9069 ± 4.2227*	1696.694 ± 5.2383*
	5	1736.0180 ± 0.7185	1735.858 ± 0.5909	1736.6183 ± 1.7285	1733.0317 ± 2.6021*	1730.7879 ± 5.1212*	1716.0428 ± 6.2719*

Table 3 The optimal threshold values obtained by BMO-DE, PSO-DE, GA, PSO, BF and MBF based Kapur's entropy methods for different threshold levels (c = 2,3,4,5)

Test images	c	BMO-DE	PSO-DE	MBF	BF	PSO	GA
Lena	2	97,164	100,165	97,164	97,164	99,165	104,167
	3	24,97,164	35,105,169	89,139,176	88,142,188	86,151,180	72,151,180
	4	24,81,125,174	24,81,128,177	78,115,146,187	74,114,149,184	92,129,162,191	57,110,178,184
	5	24,65,99,138,179	24,72,112,152,187	63,94,128,163,194	64,95,128,163,194	74,115,145,170,197	96,112,151,186,198
Pepper	2	75,147	75,146	80,150	79,149	79,146	82,146
	3	61,113,165	62,113,165	78,119,171	69,100,155	104,141,180	108,127,186
	4	58,105,148,194	58,104,146,191	52,89,130,173	63,109,144,178	57,110,162,199	72,102,172,204
	5	42,77,113,153,195	42,77,113,153,195	48,86,123,160,197	54,89,131,164,197	70,116,138,166,200	77,107,124,178,209
Baboon	2	80,144	79,143	79,143	81,144	76,144	93,152
	3	44,99,153	46,100,153	55,108,156	53,112,150	72,130,181	64,151,181
	4	34,74,114,160	35,75,115,161	40,82,125,164	39,90,131,168	65,121,153,180	90,106,152,188
	5	30,67,103,138,173	31,67,103,138,173	33,70,104,137,171	38,79,113,148,180	73,110,142,166,192	96,126,150,172,197
Hunter	2	92, 179	91,179	92,179	85,179	83,179	75,178
	3	59, 117, 179	59,118,179	55,119,177	57,104,175	85,128,166	70,148,167
	4	45, 90, 133, 179	45,91,134,179	48,91,133,180	50,98,139,180	74,131,174,200	64,100,189,200
	5	42, 85, 127,172, 214	43,87,131,175,217	45,91,135,179,222	49,93,137,179,222	90,120,164,190,219	87,96,128,196,213
Cameraman	2	125,196	125,197	120,196	116,196	115,196	76,195
	3	44, 102,196	44,104,196	72,136,197	95,139,193	96,138,191	111,165,189
	4	42, 96,145,198	43,96,145,197	41,96,145,200	42,96,139,200	77,116,151,202	71,80,141,192
	5	24,62,100,146,197	25,62,99,145,197	37,71,107,145,196	42,84,115,150,198	64,95,121,156,198	66,110,169,180,209
Livingroom	2	93,174	89,172	94,175	89,170	86,175	84,171
	3	47,103, 175	48,105,176	56,127,184	71,124,173	73,158,187	74,138,160
	4	47, 99,150,196	47,99,150,195	47,95,138,185	60,104,147,189	59,124,172,202	74,137,164,175
	5	42, 83,122,163,199	42,85,123,163,199	46,89,131,165,197	47,94,134,169,200	72,97,119,158,197	60,120,148,155,200
Airplane	2	76,174	76,172	76,174	76,173	80,175	90,176
	3	73,128,182	72,128,182	66,121,182	66,124,186	72,121,191	75,110,199
	4	20,73,128,182	39,85,136,182	70,107,145,184	71,113,149,185	74,129,162,188	87,124,154,187
	5	20,69,107,145,184	20,68,107,146,186	66,96,127,158,188	68,98,131,161,187	81,118,144,167,192	95,121,141,151,196
Butterfly	2	27,1 20	42,130	96,144	97,144	95,141	93,142
	3	27,96,144	27,94,145	87,123,164	75,109,154	63,126,172	96,103,167
	4	27,83,118,152	27,82,118,157	77,105,133,166	73,97,127,157	71,113,162,184	111,149,155,173
	5	27,77,105,133,164	27,77,105,133,163	73,96,120,144,164	74,97,120,144,167	92,116,142,157,182	75,105,140,179,198

Table 4 The optimal threshold values obtained by BMO-DE, PSO-DE, GA, PSO, BF and MBF based Otsu's entropy methods for different threshold levels (c = 2,3,4,5)

Test images	c	BMO-DE	PSO-DE	MBF	BF	PSO	GA
Lena	2	92,151	94,154	93,151	92,151	94,152	91,149
	3	80,126,170	80,126,171	81,127,171	79,125,170	79,127,170	80,124,173
	4	74,113,145,180	75,113,145,180	75,114,145,180	76,117,151,182	78,112,134,175	80,126,159,185
	5	72,108,135,159,187	71,105,132,157,186	73,109,136,159,187	66,92,122,149,183	79,110,140,167,188	80,116,146,179,213
Pepper	2	68,135	68,135	71,138	73,137	76,144	84,144
	3	63,119,166	63,119,166	64,122,170	63,125,174	72,124,171	65,116,175
	4	47,86,126,169	48,87,126,169	50,89,129,172	54,89,128,171	57,92,130,172	62,108,142,177
	5	41,79,112,146,177	43,79,113,146,177	51,86,117,150,179	47,86,123,158,183	56,84,115,150,179	52,90,128,166,191
Baboon	2	97,150	98,150	97,149	98,150	96,149	98,151
	3	85,125,161	84,123,161	85,125,161	84,126,159	85,126,166	86,125,155
	4	72,106,137,168	72,107,137,168	70,104,136,167	77,109,139,169	79,105,140,174	82,122,146,173
	5	68,99,125,150,175	67,98,125,150,175	67,99,125,149,174	70,99,127,154,177	74,104,134,161,180	73,106,140,167,199
Hunter	2	51,116	51,116	51,116	51,117	52,116	51,115
	3	36,86,135	35,86,134	34,86,133	36,86,135	39,86,135	36,89,133
	4	29,69,108,145	29,69,108,145	30,72,111,146	31,80,120,152	36,84,130,157	39,93,142,163
	5	22,53,88,122,152	23,54,88,122,152	30,72,105,134,158	31,73,109,141,178	37,85,125,154,177	39,94,130,169,204
Cameraman	2	70,144	69,143	70,144	70,143	71,143	72,145
	3	57,116,154	56,115,153	57,116,154	61,118,155	71,134,166	71,143,196
	4	41,94,139,169	41,94,139,169	41,94,139,169	48,104,142,170	65,121,147,172	59,119,155,203
	5	36,83,122,149,173	36,83,123,149,173	36,82,121,148,172	40,86,125,151,174	45,78,121,146,172	51,106,141,167,194
Livingroom	2	87,145	86,144	87,145	87,146	88,145	89,155
	3	76,123,163	76,124,163	76,123,163	75,124,164	81,127,165	83,132,174
	4	56,97,132,168	57,98,133,169	56,97,132,168	64,102,134,172	69,110,143,178	71,116,150,182
	5	48,88,120,147,178	49,88,121,147,179	49,88,120,146,178	56,94,125,148,180	56,98,128,156,190	65,104,133,160,189
Airplane	2	116,174	117,174	116,174	117,175	117,174	116,175
	3	95,146,191	93,145,190	95,146,191	91,147,190	99,158,193	86,133,204
	4	88,132,174,203	88,131,173,203	88,132,174,203	84,127,169,202	84,125,168,201	71,119,164,200
	5	71,109,144,180,205	71,109,144,180,204	71,108,143,179,204	71,110,138,175,203	60,101,138,177,204	84,124,164,188,204
Butterfly	2	98,151	100,153	98,152	99,151	99,150	100,151
	3	81,118,160	81,118,159	81,117,159	78,117,162	79,119,164	74,115,155
	4	71,99,126,162	71,99,126,161	71,98,126,162	75,105,135,165	80,113,145,177	82,119,154,184
	5	71,99,125,152,180	71,98,124,152,178	72,99,125,153,180	76,104,129,154,180	75,106,129,157,180	77,107,134,171,185

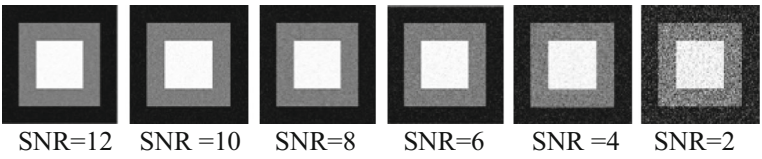

Fig. 5 Synthetic images with three layers and different SNR

We further evaluated the accuracy of the proposed BMO-DE based multilevel thresholding algorithm on synthetic images corrupted with white Gaussian noise scaled so that the signal to noise ratio (SNR) ranged from 2 to 12 according to eq. 21. Figure 5 shows a series of noisy images containing three layers with different SNR. Figure 6 shows the mean objective function values obtained using the Otsu based BMO-DE multilevel thresholding (two thresholds) algorithm for the noisy images illustrated in Fig. 5. As shown, our method performed better on noisy images with low SNR in comparison with other methods.

$$SNR = \frac{\mu_{sig}}{\delta_{sig}} \tag{21}$$

where μ_{sig} and $\delta_{sig}$are average and standard deviation of the signal values respectively.

5.3 Computation time

Table 5 shows the computational efficiency of the proposed BMO-DE algorithm for multilevel thresholding in comparison with other evolutionary algorithms in terms of average execution time (CPU time taken in seconds) over 50 runs. Compared to other evolutionary algorithms [37], the proposed BMO-DE multilevel thresholding algorithm provided lower computational time. The comparison between the run time of the Kapur and Otsu based evolutionary algorithms showed that the multilevel thresholding based on Otsu's objective function was faster.

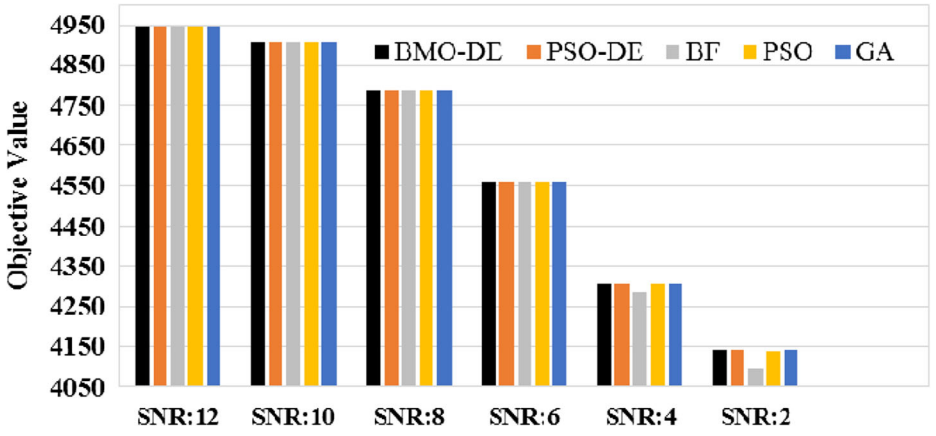

Fig. 6 Objective values for Otsu based multilevel thresholding (c = 2) for synthetic images with different SNR

Table 5 Average CPU time (sec) of BMO-DE, PSO-DE, MBF, BF, PSO and GA based algorithms each at 50 runs

Test images	c	Kapur method						Otsu method					
		BMO-DE	PSO-DE	MBF	BF	PSO	GA	BMO-DE	PSO-DE	MBF	BF	PSO	GA
Lena	2	2.9241	6.8530	6.7938	7.2063	7.8594	8.5469	1.7932	2.9388	3.0719	3.2969	3.5781	3.9688
	3	3.4802	9.2061	7.0469	7.606	8.3594	8.8594	1.8977	2.8987	3.265	3.8281	4.4031	5.2969
	4	3.8490	11.8349	7.875	8.5	9.1719	9.5156	2.0857	3.0156	4.0156	4.2188	4.75	5.6094
	5	4.4390	14.1734	8.1625	8.8125	9.4063	10.125	2.2777	3.3168	4.3719	4.7813	5.2031	5.8938
Pepper	2	4.0222	6.6008	5.725	6.5001	7.1358	8.6492	1.5570	2.8618	2.6998	2.9889	3.401	3.8569
	3	4.9989	9.2010	6.0875	6.8625	7.625	9.1056	1.7604	2.8354	3.0001	3.2157	4.3125	4.9787
	4	4.8878	11.6684	6.6046	7.4706	8.1254	9.6406	1.9667	2.8866	3.172	3.5875	4.6719	5.5156
	5	5.4532	14.1772	7.0941	7.8177	8.4844	9.9688	2.0910	3.2387	3.2219	3.6094	4.8125	5.9844
Baboon	2	1.9625	6.1485	7.2	7.625	8.0016	8.3563	1.7008	2.8978	3.1719	3.2813	3.8469	4.3969
	3	3.0705	8.6320	7.75	8.2824	8.7188	9.375	1.9150	2.9721	3.3875	3.7969	4.3125	4.7969
	4	4.0196	11.1287	8.2781	8.7188	9.1084	9.675	2.1110	3.1491	4.0469	4.2813	4.9063	5.6094
	5	4.6393	13.6482	8.5635	9.1875	9.7813	10.1875	2.2880	3.4549	4.3094	4.8206	5.3281	6.0109
Hunter	2	2.2679	6.3760	6.65	7.3594	8	8.6406	1.6889	2.9042	3.0563	3.2344	3.8438	4.4063
	3	2.7190	8.9388	7.825	8.2813	8.7031	9.9844	1.9352	3.2922	3.5594	3.9063	4.4844	4.8625
	4	3.1580	11.6237	8.125	8.7344	9.0313	9.6219	2.1850	3.3858	4.0313	4.1875	4.8125	5.3906
	5	3.6190	14.0236	9.0938	9.625	10.1406	10.6094	2.3254	3.2595	4.4563	4.8128	5.3031	6.1563
Cameraman	2	1.5632	6.0580	7.1156	7.7813	8.4844	9.25	1.7093	2.7457	2.9531	3.0625	3.4844	3.9531
	3	2.3691	8.6302	7.6625	8.272	9.0625	9.7	1.9631	2.9081	3.1219	3.6875	4.125	4.8125
	4	2.8191	11.2667	8.1219	8.5938	9.125	9.9844	2.1614	3.1039	4.0131	4.2344	4.7406	5.2500
	5	3.9591	13.7952	9.0781	9.2969	10.1094	10.9688	2.3188	3.5904	4.2844	4.6719	5.2656	6.0025
Livingroom	2	2.5990	6.6545	6.6875	6.7656	7.5844	8.2156	1.6877	3.2398	2.7656	2.8688	3.3281	3.7656
	3	3.0589	9.1591	7.1288	7.4143	8.7188	9.625	1.9171	3.1804	3.2	3.6094	4.0469	4.9531
	4	3.5389	11.9486	8.2	8.625	9.1001	9.7656	2.1359	3.4135	3.7219	4.0469	4.5	5.1056
	5	3.8589	14.5301	9.0344	9.3494	10.1719	10.5631	2.2734	3.4639	4.6594	5.003	5.7969	6.6094
Airplane	2	0.6089	5.2716	6.8563	7.3094	7.9844	8.7188	1.6615	2.9842	2.8906	3.025	3.4688	4.0000
	3	1.0898	7.7959	8	8.25	8.9688	10.4844	1.8835	2.9811	3.5656	3.8531	4.5938	5.1875
	4	1.5998	10.3453	8.1375	8.5625	9.2031	9.9531	2.1417	3.2555	3.7375	4.0125	4.7969	5.3594
	5	1.8189	12.7706	8.6906	9.0156	9.9688	10.4031	2.2917	3.3593	4.5781	4.75	5.0781	5.8125
Butterfly	2	2.5610	6.6157	7.0781	7.1719	7.7188	8.4906	1.6912	2.8249	3.1094	3.25	3.5313	3.9219
	3	3.1381	9.2992	7.7656	7.8906	8.5469	9.4656	1.9258	2.6528	3.3875	3.7188	4.1875	4.9531
	4	3.4372	12.1032	8.0906	8.4688	9	9.8659	2.1174	2.8512	4.0875	4.2031	4.8281	5.5156
	5	5.4221	15.0223	8.1313	8.6563	9.3813	10.2469	2.2938	2.8011	4.7375	5.0625	5.4594	6.1313

5.4 Advantage and disadvantage of the proposed algorithm

Multilevel thresholding using Kapur's or Otsu's algorithms is computationally expensive with increasing number of thresholds. The proposed BMO-DE-based algorithm exhibited significantly reduced computational complexity by reducing efficiently the search space.

Success of the evolutionary algorithms depends on the balance between generation of new solutions in untested regions (exploration) and concentration in the vicinity of the current good solution (exploitation) [4]. The proposed BMO-DE method provides a good balance between the exploration and exploitation parameters, which enable the algorithm to avoid local optima and achieve better performance in comparison with other algorithms.

The main limitation of the proposed segmentation method is its sensitivity to noise and intensity inhomogeneity. In these cases, the fitness function should be improved to use local information derived from neighboring pixels.

6 Conclusion

For image segmentation, the optimal thresholds in bi-level/multilevel thresholding methods can be obtained by maximizing an objective function based on some criteria such as the Otsu' criterion or Kapur's entropy, which tries to maximize the between-class variance and the posterior entropy, respectively. These methods achieve good performances for bi-level thresholding. However, by increasing the number of thresholds in multilevel thresholding, the computational complexity is increased and the segmentation accuracy might be affected be getting trapped in local extrema. Thus, a practical solution to overcome these weaknesses is to combine evolutionary methods with multilevel thresholding algorithms. In this paper, we presented a hybrid multilevel thresholding method based on the combined BMO and DE algorithms.

BMO employs distinct patterns to move through the search space without getting trapped in local extrema. It can explore the search space and generate new solutions while maintaining the population diversity. Although BMO presents promising solutions for optimization problems, it is still insufficient in terms of convergence speed and quality of solution [49]. In order to improve the quality of the BMO solution, we proposed an efficient hybrid algorithm, named BMO-DE, based on the BMO and DE algorithms. DE is easy to use, keeps a simple structure, holds acceptable convergence properties and can find the solution rapidly; however it may get trapped in local minima. By hybridization of BMO and DE, these shortcomings can be overcome. The performance of the proposed algorithm was evaluated on eight standard test images. Compared to the other well-known evolutionary algorithms including GA, PSO, BF and MBF, our algorithm achieved better results in terms of solution quality and stability. In future work, we will improve the objective function by integrating the spatial constraints and local information to further improve the accuracy of image segmentation using multilevel thresholding.

References

1. Agrawal S, Panda R, Bhuyan S, Panigrahi BKJS, Computation E (2013) Tsallis entropy based optimal multilevel thresholding using cuckoo search algorithm. 11:16–30
2. Akay BJASC (2013) A study on particle swarm optimization and artificial bee colony algorithms for multilevel thresholding. 13 (6):3066–3091

3. Ali M, Ahn CW, Pant M (2014) Multi-level image thresholding by synergetic differential evolution. Appl Soft Comput 17:1–11
4. Askarzadeh AJCNS, Simulation N (2014) Bird mating optimizer: an optimization algorithm inspired by bird mating strategies 19(4):1213–1228
5. Bayraktar Z, Komurcu M, Bossard JA, DHJItoa W (2013) propagation. The wind driven optimization technique and its application in electromagnetics 61(5):2745–2757
6. Bhandari AK, Singh VK, Kumar A, Singh GKJESwA (2014) Cuckoo search algorithm and wind driven optimization based study of satellite image segmentation for multilevel thresholding using Kapur's entropy. 41 (7):3538–3560
7. Bhandari AK, Kumar A, Singh GK (2015) Modified artificial bee colony based computationally efficient multilevel thresholding for satellite image segmentation using Kapur's, Otsu and Tsallis functions. Expert Syst Appl 42(3):1573–1601
8. Chen C, Ozolek JA, Wang W, Rohde GKJJoBI (2011) A general system for automatic biomedical image segmentation using intensity neighborhoods. 2011:8
9. Cruz-Aceves I, Aviña-Cervantes JG, López-Hernández JM, González-Reyna SEJC, medicine mmi (2013) Multiple active contours driven by particle swarm optimization for cardiac medical image segmentation. 2013
10. El Aziz MA, Ewees AA, Hassanien AEJESwA (2017) Whale Optimization Algorithm and Moth-Flame Optimization for multilevel thresholding image segmentation. 83:242–256
11. Elsayed SM, Sarker RA, Essam DLJEAoAI (2014) A new genetic algorithm for solving optimization problems. 27:57–69
12. Freixenet J, Muñoz X, Raba D, Martí J, Cufí X (2002) Yet another survey on image segmentation: Region and boundary information integration. In: European Conference on Computer Vision, Springer, pp 408–422
13. Hamdaoui F, Ladgham A, Sakly A, Mtibaa AJIJoS, Engineering IS (2016) Multi-level fractional order PSO new paradigm algorithm for image segmentation. 9 (4–5):218–225
14. Hammouche K, Diaf M, Siarry PJCV, Understanding I (2008) A multilevel automatic thresholding method based on a genetic algorithm for a fast image segmentation. 109 (2):163–175
15. Horng M-HJAM (2010) Computation. A multilevel image thresholding using the honey bee mating optimization 215(9):3302–3310
16. Horng M-HJESA (2011) Multilevel thresholding selection based on the artificial bee colony algorithm for image segmentation 38(11):13785–13791
17. Ishak ABJASC (2017) A two-dimensional multilevel thresholding method for image segmentation. 52:306–322
18. Zhao Jj, Ji Gh, Xia Y, Zhang XlJIJoB-IC (2015) Cavitary nodule segmentation in computed tomography images based on self–generating neural networks and particle swarm optimisation. 7 (1):62–67
19. Kapur JN, Sahoo PK, Wong AKJCv (1985) graphics,, processing i.A new method for gray-level picture thresholding using the entropy of the histogram. 29 (3):273–285
20. Khairuzzaman AKM, Chaudhury SJESA (2017) Multilevel thresholding using grey wolf optimizer for image segmentation 86:64–76
21. Khorram B, Yazdi M (2018) A New Optimized Thresholding Method Using Ant Colony Algorithm for MR Brain Image Segmentation.1–13
22. Lee SU, Chung SY, Park RHJCV (1990) Graphics,, Processing I A comparative performance study of several global thresholding techniques for segmentation. 52 (2):171–190
23. Li G, Zhang X, Zhao J, Zhang H, Ye J, Zhang WJTSWJ (2013) A self-adaptive parameter optimization algorithm in a real-time parallel image processing system. 2013
24. Magudeeswaran V, Ravichandran CJMPiE (2013) Fuzzy logic-based histogram equalization for image contrast enhancement. 2013
25. Maitra M, Chatterjee AJM (2008) A novel technique for multilevel optimal magnetic resonance brain image thresholding using bacterial foraging. 41 (10):1124–1134
26. Manikantan K, Arun B, Yaradoni DKSJPE (2012) Optimal multilevel thresholds based on Tsallis entropy method using golden ratio particle swarm optimization for improved image segmentation. 30:364–371
27. Niknam T, Farsani EA, Nayeripour M, Firouzi BBJEPC (2011) Systems. Hybrid fuzzy adaptive particle swarm optimization and differential evolution algorithm for distribution feeder reconfiguration 39(2):158–175
28. NJItos O (1979) man,, cybernetics. A threshold selection method from gray-level histograms. 9 (1):62–66
29. Nouri F, Kazemi K, Danyali HJMT (2018) Applications Salient object detection method using random graph. 1–19
30. Nyma A, Kang M, Kwon Y-K, Kim C-H, Kim J-MJBRI (2012) A hybrid technique for medical image segmentation. 2012
31. Pal NR, Pal SKJPr (1993) A review on image segmentation techniques. 26 (9):1277–1294
32. Panda R, Agrawal S, Bhuyan SJESA (2013) Edge magnitude based multilevel thresholding using Cuckoo search technique 40(18):7617–7628

33. Raja NSM, Kavitha G, Ramakrishnan S (2012) Analysis of vasculature in human retinal images using particle swarm optimization based Tsallis multi-level thresholding and similarity measures. In: International Conference on Swarm, Evolutionary, and Memetic Computing, Springer, pp 380–387
34. Sarkar S, Das S, Chaudhuri SS (2012) Multilevel image thresholding based on Tsallis entropy and differential evolution. In: International Conference on Swarm, Evolutionary, and Memetic Computing, Springer, pp 17–24
35. Sarkar S, Das S, Chaudhuri SSJESA (2016) Hyper-spectral image segmentation using Rényi entropy based multi-level thresholding aided with differential evolution 50:120–129
36. Sathya P, Kayalvizhi RJIJoCSI (2010) Optimum multilevel image thresholding based on tsallis entropy method with bacterial foraging algorithm. 7 (5):336
37. Sathya P, Kayalvizhi RJEAoAI (2011) Modified bacterial foraging algorithm based multilevel thresholding for image segmentation. 24 (4):595–615
38. Sathya P, Kayalvizhi RJM (2011) Amended bacterial foraging algorithm for multilevel thresholding of magnetic resonance brain images. 44 (10):1828–1848
39. Sezgin M, Sankur BJJoEi (2004) Survey over image thresholding techniques and quantitative performance evaluation. 13 (1):146–166
40. Shahvaran Z, Kazemi K, Helfroush MS, Jafarian N, Noorizadeh NJJonm (2012) Variational level set combined with Markov random field modeling for simultaneous intensity non-uniformity correction and segmentation of MR images. 209 (2):280–289
41. Shi Z, Ma J, Zhao M, Liu Y, Feng Y, Zhang M, He L, Suzuki KJBRI (2016) Many Is Better Than One: An Integration of Multiple Simple Strategies for Accurate Lung Segmentation in CT Images. 2016
42. Storn R, KJJogo P (1997) Differential evolution–a simple and efficient heuristic for global optimization over continuous spaces 11(4):341–359
43. Su Q, Hu ZJCi (2013) neuroscience, Color image quantization algorithm based on self-adaptive differential evolution. 2013:3
44. Su X, Fang W, Shen Q, Hao X (2013) An image enhancement method using the quantum-behaved particle swarm optimization with an adaptive strategy. 2013
45. TJCg P, processing i (1981) Entropic thresholding, a new approach 16(3):210–239
46. Xie L, Shen J, Han J, Zhu L, Shao L (2017) Dynamic multi-view hashing for online image retrieval. In, IJCAI
47. Yahya AA, Tan J, Hu MJAiM (2013) A novel model of image segmentation based on watershed algorithm. 2013:5
48. Zhang L, Gao Y, Xia Y, Lu K, Shen J, Ji RJITM (2014) Representative Discovery of Structure Cues for Weakly-Supervised Image Segmentation. 16 (2):470–479
49. Zhang Q, Yu G, Song HJS, Optimization, Computing I (2015) A hybrid bird mating optimizer algorithm with teaching-learning-based optimization for global numerical optimization. 3 (1):54–65

Maliheh Ahmadi received the B.Sc. degree in computer engineering from the Babol University of Technology, Babol, Iran, in 2009, and the M.Sc. degree in Artifitial Intelligence from Alzahra University, Tehran, in 2013. She is currently pursuing the Ph.D. degree from the Shiraz University of Technology. Her current research interests include biomedical signal processing, functional brain imaging, optimization methods and evolutionary algorithms.

Kamran Kazemi received his B.S. and M.S. degrees in Electrical engineering from Ferdowsi University of Mashhad and K. N. Toosi University of technology, Tehran in 2000 and 2002, respectively. He performed his Ph.D. degree in Electrical Engineering and Biomedical Engineering as cooperation between K. N. Toosi University of Technology, Tehran, Iran and University of Picardie Jules Verne (UPJV), Amiens, France. Currently he is Associate Professor in department of Electrical and Electronics Engineering, Shiraz University of Technology, Shiraz, Iran. His present interests are pattern recognition, image processing, machine learning, and mainly the application of these techniques to medical problems.

Ardalan Aarabi is an Associate Professor at the Faculty of Medicine, University of Picardie-Jules Verne (UPJV), Amiens, France. He received his B.Sc. degree in Electrical Engineering from Shiraz University, Shiraz, Iran in 1995 and his M.Sc. in Biomedical (Bioelectrical) Engineering from Iran University of Science and Technology (IUST), Tehran, Iran in 1999. He obtained his Ph.D. in Neuroscience from the University of Picardie-Jules Verne in 2007. From 2008 to 2012, he was a postdoctoral researcher at the University of Manitoba, Department of Electrical Engineering (2008–2009), MB, Canada, the University of Minnesota, Department of Biomedical Engineering (2010–2011), MN, USA, and the University of Pittsburgh, Bioengineering Department (2011–2012), PA, USA. His research interests lie in developing quantitative tools and applying biomedical signal processing and functional brain imaging methods to better understand brain dynamics and networks under pathological and physiological states in adults and neonates.

Taher Niknam received B.Sc. degree from Shiraz University, Shiraz, Iran, in 1998, and the M.Sc. and Ph.D. degrees from the Sharif University of Technology, Tehran, Iran, in 2000 and 2005, respectively, all in power electrical engineering. He is a Faculty Member with the Department of Electrical Engineering, Shiraz University of Technology, Shiraz, Iran. His current research interests include power system restructuring, impacts of distributed generations on power systems, optimization methods, and evolutionary algorithms.

Mohammad Sadegh Helfroush received the B.S. and M.S. degrees in Electrical engineering from Shiraz University of Shiraz and Sharif University of technology, Tehran in 1993 and 1995, respectively. He performed his Ph.D. degree in Electrical Engineering from Tarbiat Modarres University, Tehran, Iran. Actually he is working as Associate Professor in department of Electrical and Electronics Engineering, Shiraz University of Technology, Shiraz, Iran.